

Towards Corruption-Agnostic Robust Domain Adaptation

YIFAN XU, NLPR, Institute of Automation, Chinese Academy of Sciences & School of Artificial Intelligence, University of Chinese Academy of Sciences, China

KEKAI SHENG, Youtu Lab, Tencent Inc., China

WEIMING DONG, NLPR, Institute of Automation, Chinese Academy of Sciences & CASIA-LLvision Joint Lab, China

BAOYUAN WU, The Chinese University of Hong Kong, Shenzhen; Shenzhen Research Institute of Big Data, China

CHANGSHENG XU, NLPR, Institute of Automation, Chinese Academy of Sciences & School of Artificial Intelligence, University of Chinese Academy of Sciences, China

BAO-GANG HU, NLPR, Institute of Automation, Chinese Academy of Sciences, China

Big progress has been achieved in domain adaptation in decades. Existing works are always based on an ideal assumption that testing target domains are i.i.d. with training target domains. However, due to unpredictable corruptions (e.g., noise and blur) in real data like web images, domain adaptation methods are increasingly required to be corruption robust on target domains. In this paper, we investigate a new task, Corruption-agnostic Robust Domain Adaptation (CRDA): to be accurate on original data and robust against unavailable-for-training corruptions on target domains. This task is non-trivial due to large domain discrepancy and unsupervised target domains. We observe that simple combinations of popular methods of domain adaptation and corruption robustness have sub-optimal CRDA results. We propose a new approach based on two technical insights into CRDA: 1) an easy-to-plug module called Domain Discrepancy Generator (DDG) that generates samples that enlarge domain discrepancy to mimic unpredictable corruptions; 2) a simple but effective teacher-student scheme with contrastive loss to enhance the constraints on target domains. Experiments verify that DDG keeps or even improves performance on original data and achieves better corruption robustness than baselines.

CCS Concepts: • **Computing methodologies** → **Transfer learning**; *Unsupervised learning*; *Machine learning algorithms*; • **Computer systems organization** → *Neural networks*;

Additional Key Words and Phrases: domain adaptation, corruption robustness, transfer learning

ACM Reference Format:

Yifan Xu, Kekai Sheng, Weiming Dong, Baoyuan Wu, Changsheng Xu, and Bao-Gang Hu. 2021. Towards Corruption-Agnostic Robust Domain Adaptation. *ACM Trans. Multimedia Comput. Commun. Appl.* 1, 1, Article 1 (January 2021), 15 pages.

Authors' addresses: Yifan Xu, NLPR, Institute of Automation, Chinese Academy of Sciences & School of Artificial Intelligence, University of Chinese Academy of Sciences, 95 East Zhongguancun Rd, Beijing, China, 100190, yifan.xu@nlpr.ia.ac.cn; Kekai Sheng, Youtu Lab, Tencent Inc., Shanghai, China, saulsheng@tencent.com; Weiming Dong, NLPR, Institute of Automation, Chinese Academy of Sciences & CASIA-LLvision Joint Lab, Beijing, China, weiming.dong@ia.ac.cn; Baoyuan Wu, The Chinese University of Hong Kong, Shenzhen; Shenzhen Research Institute of Big Data, ShenZhen, China, wubaoyuan1987@gmail.com; Changsheng Xu, NLPR, Institute of Automation, Chinese Academy of Sciences & School of Artificial Intelligence, University of Chinese Academy of Sciences, Beijing, China, csxu@nlpr.ia.ac.cn; Bao-Gang Hu, NLPR, Institute of Automation, Chinese Academy of Sciences, Beijing, China, hubg@nlpr.ia.ac.cn.

Permission to make digital or hard copies of all or part of this work for personal or classroom use is granted without fee provided that copies are not made or distributed for profit or commercial advantage and that copies bear this notice and the full citation on the first page. Copyrights for components of this work owned by others than ACM must be honored. Abstracting with credit is permitted. To copy otherwise, or republish, to post on servers or to redistribute to lists, requires prior specific permission and/or a fee. Request permissions from permissions@acm.org.

© 2021 Association for Computing Machinery.

1551-6857/2021/1-ART1 \$15.00

<https://doi.org/>

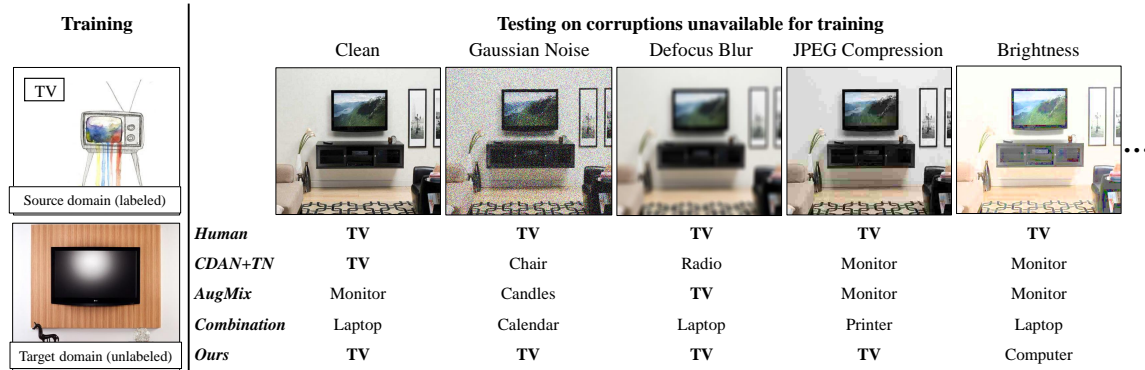


Fig. 1. Instances of corruption-agnostic robust domain adaptation (CRDA). To our surprise, existing domain adaptation method (CDAN+TN [42]) and corruption robust method (AugMix [17]), even their combination, suffer from unseen corruptions on target domain.

1 INTRODUCTION

Domain adaptation (DA) [31] is a promising technique to transfer knowledge from well-labeled source domain to assist unlabeled target domain learning with domain shift. Tremendous efforts on domain adaptation [23, 24, 26, 42] and domain generalization (DG) [20, 29, 41] indicate the significant progress on domain shift. Besides domain shift, given unpredictable corruptions (e.g., noise and blur) in real data, domain adaptation methods are increasingly required to be corruption robust on target domain (see Fig. 1). However, most DA or DG works only consider transferring source domain knowledge to some specific target datasets, while corruption robustness works [15–17, 37] usually focus on corruptions without domain shift. Thus, there is a question worth considering: *how to conduct robustness against unpredictable corruptions in cross domain scenarios?*

According to this question, we propose a new task: **Corruption-agnostic Robust Domain Adaptation (CRDA)**, i.e., DA models are required to not only achieve high performance on original target domains, but also be robust against common corruptions that are **unavailable for training**. Popular DA methods, even combining with existing corruption robustness modules, will get sub-optimal results (see Fig. 1) because they cannot handle well two challenges of CRDA: (1) unpredictable corruptions with large domain discrepancy; (2) weak constraints for robustness on unlabeled target domains. More specifically, previous augmentation robustness methods [17, 44] for corruption-agnostic robustness are always conducted in supervised scenarios with strong classification loss, which may lose effectiveness with domain discrepancy loss on target domains. We first show that after taking into domain information, we can construct more generalized augmentation in cross-domain scenarios. To our knowledge, our work is among the first attempt to unify robustness on domain shift and common corruptions.

To address the above challenges, we propose a novel mechanism towards corruption-agnostic robust domain adaptation called Domain Discrepancy Generator (DDG). Specifically, DDG generates augmentation samples that most enlarge domain discrepancy. Based on several assumptions (detailedly discussed in Section 4.1), these generated samples are proved to be able to represent unpredictable corruptions. Besides, to enhance the constraints on target domains and tackle with unstable features in the early training stage, we propose a teacher-student warm-up scheme via contrastive loss. Specifically, a teacher model is first pre-trained to learn the original representations and then a student model further distills from the teacher model to learn robustness against samples generated by DDG via contrastive loss drawn from contrastive learning [3]. Our code is available at <https://github.com/Mike9674/CRDA>.

Table 1. Comparison of related research topics.

Setting	Domain Shift	Target Domain Available	Visual Corruption
Unsupervised Domain Adaptation [23, 26, 31]	✓	✓	
Domain Generalization [20, 29, 41]	✓		
Corruption Robustness [15–17, 35]			✓
Corruption-Agnostic Robust Domain Adaptation	✓	✓	✓

Our work makes the following contributions:

- We investigate a new scenario called corruption-agnostic robust domain adaptation (CRDA) to equip domain adaptation models with corruption robustness.
- We take use of information of domain discrepancy to propose a novel module Domain Discrepancy Generator (DDG) for corruption robustness that mimic unpredictable corruptions.
- Experiments demonstrate that our method not only significantly improves corruption robustness for DA models but also maintains or even improves classification results on original target domains.

2 RELATED WORK

Unsupervised Domain Adaptation. Tremendous DA methods have made progress in cross-domain applications like recognition [12], object detection [5], and semantic segmentation [38]. The core idea is to seek domain-invariant features among source and target domains [31]. A mainstream methodology is distribution alignment, which is mainly based on Maximum Mean Discrepancy (MMD) [1, 2, 23, 25, 30] or adversarial methods [9, 11, 26, 45, 46]. Besides, some works further make improvement by pseudo-labeling [33], co-training [45], entropy regularization [36], and evolutionary-based architecture design [34]. Recently, increasing researchers focus on more realistic scenarios: considering user privacy, [22, 24] investigate the scenario where only source domain models instead of data available while training. Label corruptions in source domain [13] is proposed to address the low quality labeling problem in DA. Besides, domain generalization [20, 29, 41] aims to learn domain-invariant representations for unseen target domains. Different from existing literature (see Table 1), we propose a new and realistic topic: corruption-agnostic robust domain adaptation, which investigates corruption robustness in domain adaptation.

Corruption Robustness. Convolutional networks are proved fragile to simple corruptions by several studies [8, 19]. Assuming corruptions are known beforehand, Quality Resilient DNN [7] learns robustness against specific corruptions via a mixture of corruption-specific experts. Instead of knowing testing corruptions beforehand, we propose CRDA to learn general robustness against unseen corruptions. In recent years, increasing works begin to focus on robustness against unseen corruptions. [39] shows that fine-tuning on blurred images fails to generalize to unseen blurs. Several benchmarks [14, 15, 18, 21] are constructed to measure generalization to unseen corruptions. Self-supervised learning is found beneficial to corruption robustness [4, 16]. CutMix [43], Mixup [44], Patch Gaussian [27], Randaugment [6] and AugMix [17] are under the mainstream that aggregates several general transformations to implicitly represent unseen corruptions. However, current benchmarks and mainstream methods all take it for granted that training and testing data are from the same domain distribution, while CRDA also requires consideration of domain shift, as illustrated in Table 1. Furthermore, instead of aggregating transformations, we propose a new idea that utilize domain discrepancy information to mimic unseen corruptions.

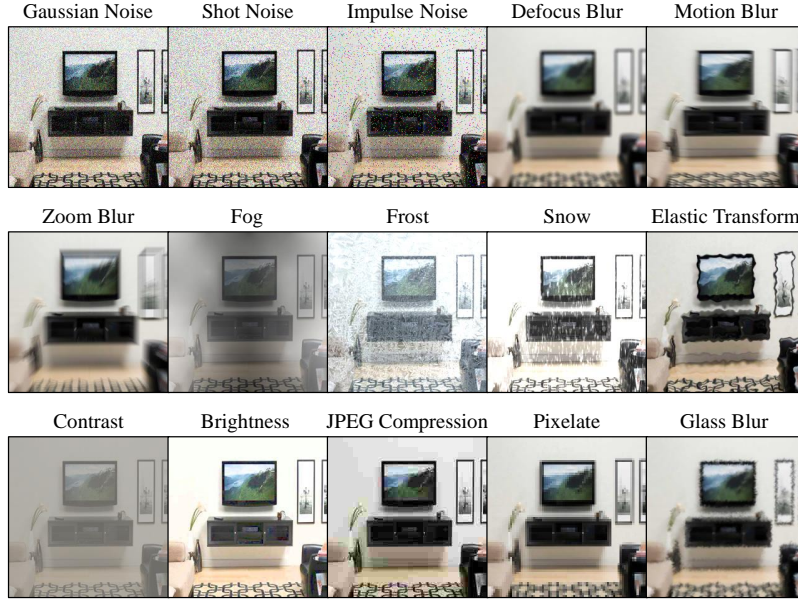


Fig. 2. Examples of 15 kinds of corruptions.

3 PRELIMINARIES

3.1 Problem definition for CRDA

In this paper, we investigate CRDA in the scope of unsupervised domain adaptation for classification. Given labeled source domain $\mathcal{D}_s = \{(\mathcal{X}_s, \mathcal{Y}_s)\}$, unlabeled target domain $\mathcal{D}_t = \{\mathcal{X}_t\}$ (\mathcal{Y}_t is unavailable while training), models are required to be robust on corrupted target domain samples $T(\mathcal{X}_t)$ while maintaining the performance on original target domain, where T denotes a corruption set **unavailable for training**. Note that $\mathcal{Y}_s = \mathcal{Y}_t = \{1, \dots, S\}$ and $P(\mathcal{D}_s) \neq P(\mathcal{D}_t)$.

3.2 Definition of corruption robustness

The concept of corruption robustness is drawn from [15] with slight modification. Given an input sample set \mathcal{X} with the corresponding label set \mathcal{Y} , a corruption set T and a model $m = f \circ c$, where f and c respectively denote a feature extractor and a classifier, the corruption robustness is measured by:

$$\mathbb{E}_{t \sim T} [\mathbb{P}_{(x,y) \sim (\mathcal{X}, \mathcal{Y})} (m(t(x)) = y)], \quad (1)$$

where we can derive the robustness by aligning features as:

$$\max \{ \mathbb{E}_{t \sim T} [\mathbb{P}_{x \sim \mathcal{X}} (f(t(x)) = f(x))] \}. \quad (2)$$

Here T denotes corruptions derived from [15], which contains 15 kinds of corruptions for T and 5 severities t for each kind (see Fig. 2).

4 METHODOLOGY

4.1 Domain Discrepancy Generator

In CRDA setting, the key challenge is that testing corruptions are unavailable during training. Besides, previous data augmentation only encourages networks to memorize the specific corruptions seen during training and leaves models unable to generalize to new corruptions [10, 39]. In this section, we attempt to utilize domain information given by domain adaptation to solve this challenge. Thus, Domain Discrepancy Generator (DDG) is proposed to generate samples that most enlarge

Algorithm 1 PGD: Projected Gradient Descent

Input: Target and source domain data x_t, x_s ; Feature extractor f ; Parameters: shift range δ , update stride η , update step number n .

Output: augmented target samples by DDG $x_t^{(DDG)}$

```

1:  $i = 0, x_t^{(DDG)} = x_t$ 
2: repeat:
3:   Transfer loss:
      $\ell = \ell_{trans}(f(x_t^{(DDG)}), f(x_s))$ 
4:   Update  $x_t^{(DDG)}$  by the gradients of transfer loss:
      $x_t^{(DDG)} \leftarrow x_t^{(DDG)} + \eta \cdot \text{sign}\left(\frac{\partial \ell}{\partial x_t^{(DDG)}}\right)$ 
5:   Clamp  $x_t^{(DDG)}$  within  $\|x_t^{(DDG)} - x_t\| \leq \delta$ 
6:    $i \leftarrow i + 1$ 
7: until  $i = n$ 
8: return  $x_t^{(DDG)}$ 

```

neighborhood of x_t , DDG generates

$$\begin{aligned}
x_t^{(DDG)} &= \arg \max_{\|x_t^{(DDG)} - x_t\| \leq \delta} \ell_{trans}(f(x_t^{(DDG)}), f(D_s)) \\
&\Rightarrow \arg \max_{t \in T} \ell_{trans}(f(t(x_t)), f(D_s)) = t_{\max}(x_t),
\end{aligned} \tag{3}$$

which means the point $x_t^{(DDG)}$ near the original target domain sample in sample space that most increases transfer loss (denoting domain discrepancy) can represent the most severe corruption. The proof of Equation (3) can be seen in the supplementary material. In practice, Domain Discrepancy Generator generates such samples via Project Gradient Descent (PGD) [28] in Algorithm 1.

It is worthy noting that the generated samples look similar to adversarial samples [28]. However, there exists few evidence that domain discrepancy could help corruption robustness in cross domain scenarios like domain adaptation ever before. We first show that it significantly improves corruption robustness on the basis of the bridge between corruptions and domain discrepancy constructed by Equation (3). Meanwhile, DDG works in an unsupervised way while common adversarial training always needs ground-truth labels.

4.2 Overall Learning Framework

The last question is how to learn robustness in unlabeled target domains. Since there is no strong constraints like classification loss in target domains, simply merging samples generated by DDG with the original data may lose the effectiveness. Thus, we utilize contrastive loss [3] to enhance the constraints on target domains. The core idea is simple, *i.e.*, minimizing the feature distance between corrupted samples with their original versions. Besides, to tackle with the unstable features in the early training stage, we further propose a warm-up scheme like teacher-student framework. The teacher model is first trained to extract the original features, while the student model then extracts corrupted features to minimize the distance to corresponding original features. Algorithm 2 shows the overall process of DDG. The proposed contrastive loss is introduced as followed.

Algorithm 2 Overall process for Domain Discrepancy Generator

Input: Data and source labels: $\mathcal{X}_s, \mathcal{X}_t, \mathcal{Y}_s$; Original DA model $f + c$; Parameters: $\delta = 60/255, \eta > 2\delta$,

$n = 2$

Output: Robust student model $f^{(stu)} + c^{(stu)}$

1: Train the original model as a teacher model $f^{(tea)} + c^{(tea)}$. Fix the parameters.

2: Construct a student network $f^{(stu)} + c^{(stu)}$ with same structure of $f + c$.

3: **repeat:**

4: Draw x_s, x_t, y_s from $\mathcal{X}_s, \mathcal{X}_t, \mathcal{Y}_s$.

5: Generate augmentation samples according to Equation (3) and Algorithm 1:

$$x_t^{(DDG)} = \text{PGD} \left(x_t, x_s, f^{(stu)}, \delta, \eta, n \right)$$

6: Update $f^{(stu)} + c^{(stu)}$ according to Equation (10).

7: **until** Convergence

8: **return** $f^{(stu)} + c^{(stu)}$

Given a batch of samples $\{x_i\}_1^N$, we use feature extractor $f^{(tea)}$ and $f^{(stu)}$ introduced in Algorithm 2 to get $2N$ representation feature vectors:

$$\begin{aligned} Z^{(tea)} &= \left\{ z_i^{(tea)} \mid z_i^{(tea)} = f^{(tea)}(x_i) \right\}_1^N, \\ Z^{(stu)} &= \left\{ z_i^{(stu)} \mid z_i^{(stu)} = f^{(stu)}(x_i) \right\}_1^N, \end{aligned} \quad (4)$$

where we define $Z = Z^{(tea)} \cup Z^{(stu)} = \{z_i\}_1^{2N}$. The similarity loss of each two features can be calculated by:

$$\ell_{sim}(z_i, z_j) = -\log \frac{\exp(\text{sim}(z_i, z_j) / \tau)}{\sum_{z_k \in Z, z_k \neq z_i} \exp(\text{sim}(z_i, z_k) / \tau)}, \quad (5)$$

where $\tau = 0.2$ is a temperature controller to control the similarity extent, and $\text{sim}(z_i, z_j) = z_i^T z_j / |z_i| |z_j|$ is cosine distance between two vectors. Note that Equation (5) is asymmetric between z_i, z_j . The final contrastive loss is defined by:

$$\ell_{con}(Z^{(stu)}, Z^{(tea)}) = \frac{1}{2N} \sum_{i=1}^N \left[\ell_{sim}(z_i^{(stu)}, z_i^{(tea)}) + \ell_{sim}(z_i^{(tea)}, z_i^{(stu)}) \right], \quad (6)$$

where the goal is to minimize the distance between feature representations $z_i^{(stu)}$ and $z_i^{(tea)}$ of a same sample x_i . The other kinds of losses defined by the original DA models ℓ_{ori} , usually containing source domain classification loss ℓ_{cls} and transfer loss ℓ_{trans} in Equation (7), also need to be calculated:

$$\ell_{ori}(x_s, x_t, y_s) = \ell_{cls}(x_s, y_s) + \ell_{trans}(x_s, x_t). \quad (7)$$

In fact, contrastive loss does not make $Z^{(stu)}$ definitely same as $Z^{(tea)}$. And thanks to corruptions, the final feature representation $Z^{(stu)}$ has a further distillation on the basis of the teacher model, which may lead to not only improvement on robustness but also better performance on domain invariance.

By utilizing the contrastive loss in Equation (6), we can minimize feature distance between samples $x_t^{(DDG)}$ generated by DDG and original samples x_t in the target domain iteratively, which leads to features of the most severely corrupted images come closer to original ones, as:

$$\min d_f \left(f(x_t^{(DDG)}), f(x_t) \right) \Rightarrow \min d_f \left(f(t_{max}(x_t)), f(x_t) \right). \quad (8)$$

In practice, Equation (8) is realized by minimizing:

$$\ell_{con}^{(DDG)}(x_t^{(DDG)}, x_t) = \ell_{con}(f^{(stu)}(x_t^{(DDG)}), f^{(tea)}(x_t)), \quad (9)$$

Together with the loss defined by the original DA model ℓ_{ori} illustrated in Equation (7) and Fig. 3, the final total loss is:

$$\ell_{total} = \ell_{ori}(x_s, x_t, y_s) + \lambda \ell_{con}^{(DDG)}(x_t^{(DDG)}, x_t). \quad (10)$$

Note that DDG only generated samples on target domains and the generated samples are only processed by contrastive loss.

4.3 Further Explanation

Intuitively, DDG should loop many times like $n = 10$ in PGD to generates an augmented sample, which is time-consuming. In this section, we theoretically show that we only need to consider the edge point so that by setting $n = 2$ is enough, which effectively reduces the time consumption. We begin with the following proposition.

PROPOSITION 1. *Only aligning the edge points $\{x_t^{(DDG)} \mid \|x_t^{(DDG)} - x_t\| = \delta\}$ around the δ neighborhood in Equation (3) is enough to gain corruption robustness under the DDG framework.*

Given input data x , a feature extractor f and a corruption T with continuous severity, we denote the distance in feature space $d_f(f(T(x)), f(x))$ as $d(T)$. Then Assumption 2 can be explained as T is positively correlated with $d(T)$. Due to the properties of monotonic function, the upper bound of $d(T)$ is $d(T_{max})$:

$$0 \leq d(T) \leq d(T_{max}) = d_{max}, \quad (11)$$

where T_{max} denotes the most severe level of corruption T . By limiting d_{max} to 0, we get:

$$\lim_{d_{max} \rightarrow 0} d(T) = \lim_{d_{max} \rightarrow 0} d_f(f(T(x)), f(x)) = 0, \quad (12)$$

which means for all severity levels of corruption T , features of corrupted data $T(x)$ and clean data x are the same when $d_{max} \rightarrow 0$. Thus, robustness against a specific corruption is achieved.

Now the last issue is how to limit d_{max} to 0. Note that:

$$d_{max} = d(T_{max}) = d_f(f(T_{max}(x)), f(x)). \quad (13)$$

Thus, by aligning features of the most severely corrupted samples $T_{max}(x)$ with original features x , we get $d_{max} \rightarrow 0$.

Considering Assumption 1, the shift in sample space increases as the increase of the severity level of a corruption T . Thus, the most severe corruption $T_{max}(x)$ is always achieved on the edge points of δ cycle. Then we can use $\{x_t^{(DDG)} \mid \|x_t^{(DDG)} - x_t\| = \delta\}$ to implicitly represent $T_{max}(x)$ due to the conclusion in Equation (3). By aligning features of these edge points with the original features via minimizing the contrastive loss defined in Equation (9), corruption robustness is achieved under DDG as :

$$\lim_{\ell_{con}^{(DDG)} \rightarrow 0} d(T) = \lim_{\ell_{con}^{(DDG)} \rightarrow 0} d_f(f(T(x)), f(x)) = 0. \quad (14)$$

Proposition 1 is derived.

Thus, by setting stride η bigger than range 2δ , we can reach the edge point in one step. In practice, only step $n = 2$ gains enough good performance.

4.4 Metrics for corruption robustness

The commonly used standardized aggregate performance measure is the Corruption Error (CE) [15], which can be computed by:

$$CE_T^f = \left(\sum_{t=1}^5 E_{t,T}^f \right) / \left(\sum_{t=1}^5 E_{t,T}^{AlexNet} \right), \quad (15)$$

where $E_{t,T}^f$ denotes the error rate of model f on target domain data transformed by corruption T with severity t . The *AlexNet* is trained on clean source domain and tested on corrupted target domain.

The corruption robustness of model f is summarized by averaging Corruption Error values of 15 corruptions introduced in Section 3.2: $CE_{\text{Gaussian Noise}}^f, \dots, CE_{\text{Glass Blur}}^f$. The results in the mean CE or mCE [15] for short. mCE is calculated by only one setting (e.g., the Ar:Rw setting in Office-Home). For average performance of corruption robustness on the whole dataset (e.g., Office-Home), we need to average mCE values of all settings.

5 EXPERIMENTS

5.1 Setups

Datasets. Office-Home and Office-31 are two benchmark datasets widely adopted for visual domain adaptation algorithms. Experiments are mainly conducted on Office-Home, a relatively challenging dataset. *Office-Home* [40] is a challenging medium sized benchmark, which contains 15588 images from 4 domains (Artistic images (Ar), Clip Art (Cl), Product images (Pr), and Real-World images (Rw)). Each domain consists of 65 object classes under daily life environment. *Office-31* [32] is a standard benchmark with 4110 images and 31 classes under office environment. There are totally three domains: Amazon (A), Webcam (W) and DSLR (D).

Corruption. To check the corruption robust of one given DA model, we create the corrupted version of Office-31 and Office-Home by using the corruption types defined by ImageNet-C [15], a widely used benchmark for corruption robustness. For each image, there exists 15 corruption types with 5 levels of severity as illustrated in Fig. 2.

Baselines. To illustrate the improvement on CRDA, we apply our method to **CDAN+TN** [26, 42], a classic baseline model for domain adaptation. We further apply our method to a SOTA DA model **DCAN** [23]. Note that the domain discrepancies of CDAN+TN and DCAN are respectively measured by adversarial methods [11] and MMD [1]. We compare our DDG method with **AugMix** [17], a SOTA method for corruption robustness, which aggregates several general transformations such as contrast, equalization and posterization for data augmentation.

Implementation details. For contrastive loss in Equations (10), the trade-off λ is set to 0.5. For DDG, we conduct Algorithm 2 with $\delta = 60/255$, $\eta = 6$, $n = 2$. Network structures and other hyper-parameters are the same as the original DA models.

5.2 Experiments in CRDA

We compare DDG with AugMix and the original DA models on both corruption robustness and original performance. In addition, we further set an empirical lower bound for CRDA calculated by simply replacing DDG-generated samples in Algorithm 2 with corresponding corrupted samples, which means models that reach the lower bound can be robust against unpredictable corruptions as if they are already known beforehand.

Table 2. Accuracy (%) on clean Office-Home data (ResNet-50).

Method	Ar→Cl	Ar→Pr	Ar→Rw	Cl→Ar	Cl→Pr	Cl→Rw	Pr→Ar	Pr→Cl	Pr→Rw	Rw→Ar	Rw→Cl	Rw→Pr	Avg (†)
ResNet	34.9	50.0	58.0	37.4	41.9	46.2	38.5	31.2	60.4	53.9	41.2	59.9	46.1
DAN	43.6	57.0	67.9	45.8	56.5	60.4	44.0	43.6	67.7	63.1	51.5	74.3	56.3
DANN	45.6	59.3	70.1	47.0	58.5	60.9	46.1	43.7	68.5	63.2	51.8	76.8	57.6
JAN	45.9	61.2	68.9	50.4	59.7	61.0	45.8	43.4	70.3	63.9	52.4	76.8	58.3
DWT	50.3	72.1	77.0	59.6	69.3	70.2	58.3	48.1	77.3	69.3	53.6	82.0	65.6
CDAN	50.7	70.6	76.0	57.6	70.0	70.0	57.4	50.9	77.3	70.9	56.7	81.6	65.8
TADA	53.1	72.3	77.2	59.1	71.2	72.1	59.7	53.1	78.4	72.4	60.0	82.9	67.6
SymNets	47.7	72.9	78.5	64.2	71.3	74.2	64.2	48.8	79.5	74.5	52.6	82.7	67.6
MDD	54.9	73.7	77.8	60.0	71.4	71.8	61.2	53.6	78.1	72.5	60.2	82.3	68.1
CDAN+TN	54.1	70.3	77.9	62.2	74.4	73.7	62.4	53.1	81.0	72.8	56.9	82.5	68.4
+AugMix	50.5	70.1	74.9	56.7	69.6	68.7	53.9	50.4	75.9	67.9	58.2	80.6	64.8
+DDG	57.1	74.4	79.4	63.5	75.9	75.3	63.2	54.9	81.9	73.1	58.8	84.2	70.1
DCAN	57.8	76.3	82.9	68.5	72.7	76.7	68.0	56.5	82.1	73.5	60.8	83.3	71.6
+AugMix	55.8	74.8	82.5	67.6	72.1	76.1	67.5	55.0	82.5	73.4	59.0	82.5	70.7
+DDG	58.1	75.2	82.9	68.7	75.0	77.6	68.1	56.6	81.8	73.9	60.6	83.1	71.8

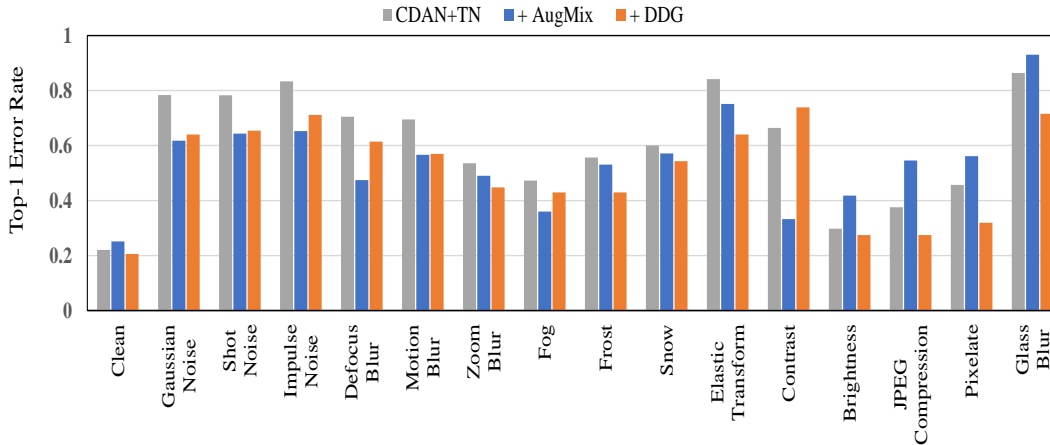


Fig. 4. Error rate (%) on Ar→Rw of Office-Home for different corruptions with the most severe level under CRDA (ResNet-50).

Fig. 4 shows the error rate on clean data and 15 different corruptions with the most severe severity in a single setting. It is reported that DDG achieves improvement over most kinds of corruptions with about 10 percentages in average than the original model and 3 percentages than AugMix. We observe that AugMix only achieves relatively high robustness on several corruptions such as Fog and Contrast. The reason possibly is that these corruptions can be implied by the aggregation of the general transformations defined by AugMix, however, corruptions like Pixelate may lie out of the implied set. Instead, our DDG achieves a much more generalizable implied set thanks to reasonable utilization of domain discrepancy information. It is worthy of noting that DDG can also improve the original accuracy, which is detailedly reported in Table 2.

Fig. 4 also shows that DDG gains no improvement over the Contrast corruption. We argue the reason probably is that this corruption conducts too much shift in sample space which goes beyond the scope of Assumption 1. Possible solutions include loosening the constraint in Assumption 1 and considering the invariant order of pixel values (Contrast does not change the order of pixel values). We leave them for future work.

We report the overall robustness under the whole Office-Home and Office-31 datasets in Table 3 and Table 4 with the standard robustness metric mCE. Results show that even the SOTA model

Table 3. mCE (%) on all cross-domain settings of Office-Home dataset under CRDA (ResNet-50).

Settings	CDAN+TN			DCAN			Lower Bound
	-	AugMix	Ours	-	AugMix	Ours	
Ar→Cl	69.7	69.3	59.8	61.4	63.2	58.3	52.2
Ar→Pr	62.2	52.8	52.2	51.0	49.3	48.0	37.7
Ar→Rw	59.2	56.0	48.0	47.9	46.0	44.6	30.8
Cl→Ar	65.4	73.7	66.0	58.6	57.4	55.2	45.8
Cl→Pr	58.7	56.6	51.9	58.0	57.3	51.6	34.6
Cl→Rw	57.6	61.3	56.2	52.0	53.8	47.5	34.7
Pr→Ar	65.5	72.2	63.6	61.1	58.9	55.1	44.7
Pr→Cl	70.9	71.4	63.6	66.2	65.3	62.2	54.9
Pr→Rw	55.0	55.3	48.8	53.7	48.5	49.4	25.7
Rw→Ar	63.2	62.4	57.8	63.0	59.2	57.7	36.0
Rw→Cl	70.4	61.4	64.4	64.0	64.2	59.9	52.9
Rw→Pr	60.9	52.6	47.9	58.4	52.5	52.6	26.8
Avg (↓)	63.2	62.1	56.7	57.9	56.3	53.5	39.7

Table 4. mCE (%) on all cross-domain settings of Office-31 dataset under CRDA (ResNet-50).

Settings	CDAN+TN			DCAN			Lower Bound
	-	AugMix	Ours	-	AugMix	Ours	
A→D	60.3	46.0	48.9	42.3	40.5	36.9	12.3
A→W	59.6	65.2	46.9	40.0	32.4	28.6	10.1
D→A	64.1	66.0	62.4	50.3	53.0	46.6	33.8
D→W	83.5	59.9	69.7	45.2	48.1	35.9	4.6
W→A	64.7	67.9	60.1	60.1	59.8	55.0	36.4
W→D	120.2	64.3	70.9	46.6	54.6	44.5	0.7
Avg (↓)	75.4	61.6	59.8	47.4	48.1	41.3	16.3

Table 5. mCE (%) on Ar→Rw for different update strides η in DDG

δ	η	n	mCE (↓)
60/255	$> 2\delta$	2	48.0
60/255	$> 2\delta$	10	49.6
60/255	15/255	10	51.6
60/255	6/255	10	52.8

AugMix has sub-optimal results or even worse performance in some settings, which indicates the challenge of CRDA. Despite the challenging task, DDG still gains improvement with obvious margins. Meanwhile, there is still a long way for further study to reach the lower bound in CRDA. Besides robustness, DDG also maintains or improves the original accuracy of DA models. Results are shown in Table 2.

5.3 Empirical analysis

Ablation. In Section 4.3, we theoretically show only considering the edge points on the δ cycle is enough for DDG, which is realized by setting stride $\eta > 2\delta$ in Algorithm 2. Table 5 reports the mCE under CRDA with different strides η . Results show that the setting $\eta > 2\delta$, which results in only considering the edge points, gains best performance. We conclude the reason why settings $\eta \ll \delta$ perform relatively poorer is that they may wander in the δ cycle instead of reaching the large-shift

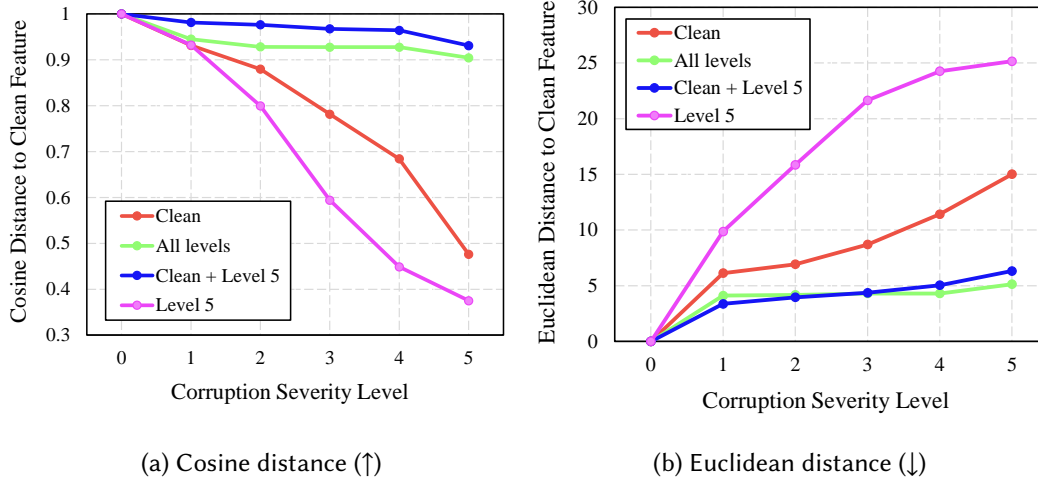


Fig. 5. Feature distance between a clean image and the versions corrupted by five severity levels of Gaussian Noise on the basis of different models: **Clean** (a ResNet-50 trained on clean data), **All levels** (trained on all severity levels of Gaussian Noise), **Clean + Level 5** (trained on clean data and severity level 5 Gaussian Noise), **Level 5** (trained on data only corrupted by severity level 5).

Table 6. Error rate (%) under a specific known corruption on the Ar→Rw setting of Office-Home dataset for teacher-student warm-up scheme.

Corruption	CDAN+TN			Corruption	CDAN+TN		
	-	DataAug	Ours		-	DataAug	Ours
Clean	22.1	24.6	21.2	Frost	55.7	30.6	25.5
Gaussian Noise	78.4	33.4	27.8	Snow	60.0	31.2	23.9
Shot Noise	78.3	34.9	26.9	Elastic Transform	84.2	30.0	23.3
Impulse Noise	83.4	33.4	24.4	Contrast	66.4	24.6	23.0
Defocus Blur	70.4	34.9	26.7	Brightness	29.7	26.5	23.6
Motion Blur	69.5	28.4	24.3	JPEG Compression	37.6	29.0	23.2
Zoom Blur	53.6	29.4	23.1	Pixelate	45.7	26.9	22.6
Fog	47.3	24.6	23.6	Glass Blur	86.4	37.0	27.8

points on the edge, which causes a lack of consideration on large-shift corruptions like contrast and blurs. Table 5 also shows that only 2 update steps is enough for DDG to gain corruption robustness. More ablation results can be seen in Appendix.

Teacher-student warm-up scheme. In this section, we aim to evaluate the effectiveness of the teacher-student warm-up scheme. To compare with simply augmenting samples with testing corruptions, we replace DDG-generated samples in Algorithm 2 with corresponding testing corruptions. Table 6 precisely reports the error rate on original data and corruptions with the most severe severity. Results show that our warm-up scheme can significantly improve the model’s robustness against a specific corruption. Furthermore, our scheme can further improve the model’s original performance instead of negative effect brought by pure data augmentation. In another word, the teacher-student warm-up scheme does not conduct trade-off over robustness and accuracy.

Order-invariant representations of corruptions. We empirically observe that the distance between the corrupted versions and the corresponding clean image in feature space (**feature distance** for

precise) is always positively correlated to the severity of corruptions. Training details are shown in the supplementary material. Fig. 5 shows that even only trained on clean and corrupted samples with a single severity (Clean + Level 5), models still learn the positive correlation instead of relatively nearer feature distance on a specific severity. In a word, networks always learn order-invariant representations in feature space for different levels of severity, which contributes to Assumption 2 in Section 4.1.

6 CONCLUSION

In this paper, we throw a new sight to domain adaptation to investigate a more realistic new task, Corruption-agnostic Robust Domain Adaptation (CRDA). Taking domain information into consideration, we present a new idea for corruption robustness called Domain Discrepancy Generator (DDG) that mimic unpredictable corruptions via generating samples most enlarging domain discrepancy. Besides, we propose a teacher-student warm-up scheme via contrastive loss to enhance the constraints on unlabelled target domains and stabilize the early training stage feature. Empirical results justify that DDG outperforms existing baselines on original accuracy and achieves better corruption robustness.

REFERENCES

- [1] Karsten M Borgwardt, Arthur Gretton, Malte J Rasch, Hans-Peter Kriegel, Bernhard Schölkopf, and Alex J Smola. 2006. Integrating structured biological data by kernel maximum mean discrepancy. *Bioinformatics* 22, 14 (2006), e49–e57.
- [2] Chao Chen, Zhihong Chen, Boyuan Jiang, and Xinyu Jin. 2019. Joint domain alignment and discriminative feature learning for unsupervised deep domain adaptation. In *Proceedings of the AAAI Conference on Artificial Intelligence*, Vol. 33. 3296–3303.
- [3] Ting Chen, Simon Kornblith, Mohammad Norouzi, and Geoffrey Hinton. 2020. A simple framework for contrastive learning of visual representations. In *ICML*.
- [4] Tianlong Chen, Sijia Liu, Shiyu Chang, Yu Cheng, Lisa Amini, and Zhangyang Wang. 2020. Adversarial Robustness: From Self-Supervised Pre-Training to Fine-Tuning. In *Proceedings of the IEEE/CVF Conference on Computer Vision and Pattern Recognition*. 699–708.
- [5] Yuhua Chen, Wen Li, Christos Sakaridis, Dengxin Dai, and Luc Van Gool. 2018. Domain adaptive faster r-cnn for object detection in the wild. In *Proceedings of the IEEE conference on computer vision and pattern recognition*. 3339–3348.
- [6] Ekin D Cubuk, Barret Zoph, Jonathon Shlens, and Quoc V Le. 2020. Randaugment: Practical automated data augmentation with a reduced search space. In *Proceedings of the IEEE/CVF Conference on Computer Vision and Pattern Recognition Workshops*. 702–703.
- [7] Samuel Dodge and Lina Karam. 2017. Quality resilient deep neural networks. *arXiv preprint arXiv:1703.08119* (2017).
- [8] Samuel Dodge and Lina Karam. 2017. A study and comparison of human and deep learning recognition performance under visual distortions. In *2017 26th international conference on computer communication and networks (ICCCN)*. IEEE, 1–7.
- [9] Yaroslav Ganin, Evgeniya Ustinova, Hana Ajakan, Pascal Germain, Hugo Larochelle, François Laviolette, Mario Marchand, and Victor Lempitsky. 2016. Domain-adversarial training of neural networks. *The Journal of Machine Learning Research* 17, 1 (2016), 2096–2030.
- [10] Robert Geirhos, Carlos RM Temme, Jonas Rauber, Heiko H Schütt, Matthias Bethge, and Felix A Wichmann. 2018. Generalisation in humans and deep neural networks. In *Advances in neural information processing systems*. 7538–7550.
- [11] Ian Goodfellow, Jean Pouget-Abadie, Mehdi Mirza, Bing Xu, David Warde-Farley, Sherjil Ozair, Aaron Courville, and Yoshua Bengio. 2014. Generative adversarial nets. In *Advances in Neural Information Processing Systems (NIPS)*. 2672–2680.
- [12] Raghuraman Gopalan, Ruonan Li, and Rama Chellappa. 2011. Domain adaptation for object recognition: An unsupervised approach. In *2011 international conference on computer vision*. IEEE, 999–1006.
- [13] Zhongyi Han, Xian-Jin Gui, Chaoran Cui, and Yilong Yin. 2020. Towards Accurate and Robust Domain Adaptation under Noisy Environments. In *Proceedings of the Twenty-Ninth International Joint Conference on Artificial Intelligence, IJCAI-20*, Christian Bessiere (Ed.). IJCAI, 2269–2276. Main track.
- [14] Dan Hendrycks, Steven Basart, Norman Mu, Saurav Kadavath, Frank Wang, Evan Dorundo, Rahul Desai, Tyler Zhu, Samyak Parajuli, Mike Guo, Dawn Song, Jacob Steinhardt, and Justin Gilmer. 2020. The Many Faces of Robustness: A Critical Analysis of Out-of-Distribution Generalization. *arXiv preprint arXiv:2006.16241* (2020).

- [15] Dan Hendrycks and Thomas Dietterich. 2019. Benchmarking neural network robustness to common corruptions and perturbations. In *ICLR*.
- [16] Dan Hendrycks, Mantas Mazeika, Saurav Kadavath, and Dawn Song. 2019. Using self-supervised learning can improve model robustness and uncertainty. In *Advances in Neural Information Processing Systems*. 15663–15674.
- [17] Dan Hendrycks, Norman Mu, Ekin D Cubuk, Barret Zoph, Justin Gilmer, and Balaji Lakshminarayanan. 2020. Augmix: A simple data processing method to improve robustness and uncertainty. In *Augmix: A simple data processing method to improve robustness and uncertainty (ICLR)*.
- [18] Dan Hendrycks, Kevin Zhao, Steven Basart, Jacob Steinhardt, and Dawn Song. 2019. Natural Adversarial Examples. *arXiv preprint arXiv:1907.07174* (2019).
- [19] Hossein Hosseini, Baicen Xiao, and Radha Poovendran. 2017. Google’s cloud vision api is not robust to noise. In *2017 16th IEEE International Conference on Machine Learning and Applications (ICMLA)*. IEEE, 101–105.
- [20] Zeyi Huang, Haohan Wang, Eric P. Xing, and Dong Huang. 2020. Self-Challenging Improves Cross-Domain Generalization. In *ECCV*.
- [21] Daniel Kang, Yi Sun, Dan Hendrycks, Tom Brown, and Jacob Steinhardt. 2019. Testing robustness against unforeseen adversaries. *arXiv preprint arXiv:1908.08016* (2019).
- [22] Rui Li, Qianfen Jiao, Wenming Cao, Hau-San Wong, and Si Wu. 2020. Model Adaptation: Unsupervised Domain Adaptation without Source Data. In *Proceedings of the IEEE/CVF Conference on Computer Vision and Pattern Recognition*. 9641–9650.
- [23] Shuang Li, Chi Harold Liu, Qiuxia Lin, Binhui Xie, Zhengming Ding, Gao Huang, and Jian Tang. 2020. Domain Conditioned Adaptation Network. In *Thirty-Fourth AAAI Conference on Artificial Intelligence (AAAI-20)*.
- [24] Jian Liang, Dapeng Hu, and Jiashi Feng. 2020. Do We Really Need to Access the Source Data? Source Hypothesis Transfer for Unsupervised Domain Adaptation. In *International Conference on Machine Learning (ICML)*. xx–xx.
- [25] Mingsheng Long, Yue Cao, Jianmin Wang, and Michael Jordan. 2015. Learning transferable features with deep adaptation networks. In *International conference on machine learning*. PMLR, 97–105.
- [26] Mingsheng Long, Zhangjie Cao, Jianmin Wang, and Michael I Jordan. 2018. Conditional adversarial domain adaptation. In *Advances in Neural Information Processing Systems*. 1640–1650.
- [27] Raphael Gontijo Lopes, Dong Yin, Ben Poole, Justin Gilmer, and Ekin D Cubuk. 2019. Improving robustness without sacrificing accuracy with patch gaussian augmentation. *arXiv preprint arXiv:1906.02611* (2019).
- [28] Aleksander Madry, Aleksandar Makelov, Ludwig Schmidt, Dimitris Tsipras, and Adrian Vladu. 2018. Towards deep learning models resistant to adversarial attacks. In *ICLR*.
- [29] Toshihiko Matsuura and Tatsuya Harada. 2020. Domain Generalization Using a Mixture of Multiple Latent Domains. In *AAAI*.
- [30] Sinno Jialin Pan, Ivor W Tsang, James T Kwok, and Qiang Yang. 2010. Domain adaptation via transfer component analysis. *IEEE Transactions on Neural Networks* 22, 2 (2010), 199–210.
- [31] Sinno Jialin Pan and Qiang Yang. 2009. A survey on transfer learning. *IEEE Transactions on knowledge and data engineering* 22, 10 (2009), 1345–1359.
- [32] Kate Saenko, Brian Kulis, Mario Fritz, and Trevor Darrell. 2010. Adapting visual category models to new domains. In *ECCV*.
- [33] Kuniaki Saito, Yoshitaka Ushiku, and Tatsuya Harada. 2017. Asymmetric tri-training for unsupervised domain adaptation. *arXiv preprint arXiv:1702.08400* (2017).
- [34] Kekai Sheng, Ke Li, Xiawu Zheng, Jian Liang, Weiming Dong, Feiyue Huang, Rongrong Ji, and Xing Sun. 2021. On Evolving Attention Towards Domain Adaptation. *arXiv preprint arXiv:2103.13561* (2021).
- [35] Connor Shorten and Taghi M Khoshgoftaar. 2019. A survey on image data augmentation for deep learning. *Journal of Big Data* 6, 1 (2019), 60.
- [36] Rui Shu, Hung H Bui, Hirokazu Narui, and Stefano Ermon. 2018. A dirt-t approach to unsupervised domain adaptation. In *ICLR*.
- [37] Yu Sun, Xiaolong Wang, Liu Zhuang, John Miller, Moritz Hardt, and Alexei A. Efros. 2020. Test-Time Training with Self-Supervision for Generalization under Distribution Shifts. In *ICML*.
- [38] Yi-Hsuan Tsai, Wei-Chih Hung, Samuel Schulter, Kihyuk Sohn, Ming-Hsuan Yang, and Manmohan Chandraker. 2018. Learning to adapt structured output space for semantic segmentation. In *Proceedings of the IEEE Conference on Computer Vision and Pattern Recognition*. 7472–7481.
- [39] Igor Vasiljevic, Ayan Chakrabarti, and Gregory Shakhnarovich. 2016. Examining the impact of blur on recognition by convolutional networks. *arXiv preprint arXiv:1611.05760* (2016).
- [40] Hemanth Venkateswara, Jose Eusebio, Shayok Chakraborty, and Sethuraman Panchanathan. 2017. Deep hashing network for unsupervised domain adaptation. In *CVPR*.
- [41] Riccardo Volpi, Hongseok Namkoong, Ozan Sener, John C Duchi, Vittorio Murino, and Silvio Savarese. 2018. Generalizing to unseen domains via adversarial data augmentation. In *Advances in neural information processing systems*.

- 5334–5344.
- [42] Ximei Wang, Ying Jin, Mingsheng Long, Jianmin Wang, and Michael I Jordan. 2019. Transferable normalization: Towards improving transferability of deep neural networks. In *Advances in Neural Information Processing Systems*. 1953–1963.
 - [43] Sangdoon Yun, Dongyoon Han, Seong Joon Oh, Sanghyuk Chun, Junsuk Choe, and Youngjoon Yoo. 2019. Cutmix: Regularization strategy to train strong classifiers with localizable features. In *Proceedings of the IEEE International Conference on Computer Vision*. 6023–6032.
 - [44] Hongyi Zhang, Moustapha Cisse, Yann N Dauphin, and David Lopez-Paz. 2018. mixup: Beyond empirical risk minimization. *International Conference on Learning Representations (2018)*.
 - [45] Weichen Zhang, Wanli Ouyang, Wen Li, and Dong Xu. 2018. Collaborative and adversarial network for unsupervised domain adaptation. In *Proceedings of the IEEE Conference on Computer Vision and Pattern Recognition*. 3801–3809.
 - [46] Yabin Zhang, Hui Tang, Kui Jia, and Mingkui Tan. 2019. Domain-symmetric networks for adversarial domain adaptation. In *Proceedings of the IEEE Conference on Computer Vision and Pattern Recognition*. 5031–5040.

Supplementary Material for “Towards Corruption-Agnostic Robust Domain Adaptation”

YIFAN XU, NLP, Institute of Automation, Chinese Academy of Sciences & School of Artificial Intelligence, University of Chinese Academy of Sciences, China

KEKAI SHENG, Youtu Lab, Tencent Inc., China

WEIMING DONG, NLP, Institute of Automation, Chinese Academy of Sciences & CASIA-LLvision Joint Lab, China

BAOYUAN WU, The Chinese University of Hong Kong, Shenzhen; Shenzhen Research Institute of Big Data, China

CHANGSHENG XU, NLP, Institute of Automation, Chinese Academy of Sciences & School of Artificial Intelligence, University of Chinese Academy of Sciences, China

BAO-GANG HU, NLP, Institute of Automation, Chinese Academy of Sciences, China

ACM Reference Format:

Yifan Xu, Kekai Sheng, Weiming Dong, Baoyuan Wu, Changsheng Xu, and Bao-Gang Hu. 2021. Supplementary Material for “Towards Corruption-Agnostic Robust Domain Adaptation”. *ACM Trans. Multimedia Comput. Commun. Appl.* 1, 1, Article 1 (January 2021), 6 pages.

In this supplementary material, we provide details omitted in the main manuscript, including:

- Section 1: Further explanation for the importance and challenge of the new task setting, CRDA.
- Section 2: Empirical proof for three assumptions in Section 4.1 of the main manuscript.
- Section 3: Proof for Equation (3) in the main manuscript.
- Section 4: More ablation study results.
- Section 5: Details of corruptions.
- Section 6: More details of experiments.

1 FURTHER EXPLANATION

In this section, we emphasize the challenge and importance of CRDA through the lower bound.

Authors’ addresses: Yifan Xu, NLP, Institute of Automation, Chinese Academy of Sciences & School of Artificial Intelligence, University of Chinese Academy of Sciences, 95 East Zhongguancun Rd, Beijing, China, 100190, yifan.xu@nlpr.ia.ac.cn; Kekai Sheng, Youtu Lab, Tencent Inc., Shanghai, China, saulsheng@tencent.com; Weiming Dong, NLP, Institute of Automation, Chinese Academy of Sciences & CASIA-LLvision Joint Lab, Beijing, China, weiming.dong@ia.ac.cn; Baoyuan Wu, The Chinese University of Hong Kong, Shenzhen; Shenzhen Research Institute of Big Data, ShenZhen, China, wubaoyuan1987@gmail.com; Changsheng Xu, NLP, Institute of Automation, Chinese Academy of Sciences & School of Artificial Intelligence, University of Chinese Academy of Sciences, Beijing, China, csxu@nlpr.ia.ac.cn; Bao-Gang Hu, NLP, Institute of Automation, Chinese Academy of Sciences, Beijing, China, hubg@nlpr.ia.ac.cn.

Permission to make digital or hard copies of all or part of this work for personal or classroom use is granted without fee provided that copies are not made or distributed for profit or commercial advantage and that copies bear this notice and the full citation on the first page. Copyrights for components of this work owned by others than ACM must be honored. Abstracting with credit is permitted. To copy otherwise, or republish, to post on servers or to redistribute to lists, requires prior specific permission and/or a fee. Request permissions from permissions@acm.org.

© 2021 Association for Computing Machinery.

1551-6857/2021/1-ART1 \$15.00

<https://doi.org/>

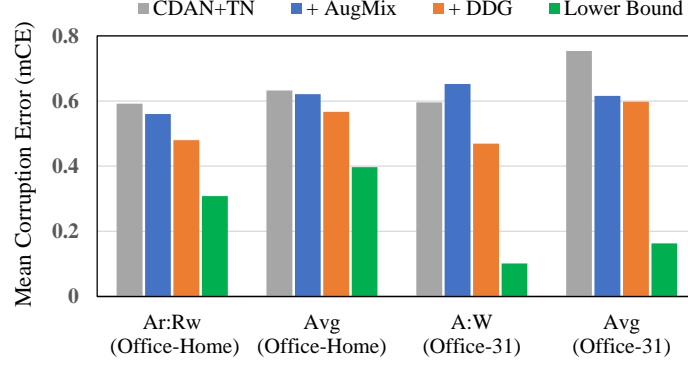


Fig. 1. mCE (%) on Office-Home and Office-31 datasets.

Corruption robustness is always an important subject. Previous works do not pay much care for corruptions because it has been addressed enough well in the setting of supervised learning. However, **corruption robustness in domain adaptation is far from satisfactory.**

As shown in Fig. 1, to estimate the status of current study, we further set an empirical lower bound for CRDA calculated by mCE of TSCL applied on CDAN+TN, which assumes testing corruptions are available while training. Models that reach the lower bound can be robust against unseen corruptions as if they are already known beforehand.

It is shown that current methods for CRDA still hold a large distance to the lower bound. In a word, instead of enough good progress in supervised learning, **there is still a long way to go for CRDA.**

2 PROOF FOR THREE ASSUMPTIONS IN SECTION 4.1 OF THE MAIN MANUSCRIPT

2.1 Proof for Assumption 1

We give the empirical proof for Assumption 1 via Average Shift. Given a clean image $x \in \mathbb{R}^{c \times w \times h}$ and a corruption t , the Average Shift is calculated by:

$$\begin{aligned}
 avg &= \frac{\|x - t(x)\|_1}{cwh} \\
 &= \frac{1}{cwh} \sum_{i=1}^c \sum_{j=1}^w \sum_{k=1}^h |(x - t(x))_{ijk}|.
 \end{aligned} \tag{1}$$

Table 1 shows the Average Shift of an image under 15 corruptions with the most severe level. It is shown that most corruptions are within the shift range $\delta = 0.26 \approx 60/255$.

Fig. 2 verifies that the Average Shift in sample space increases with the increase of the severity level of most corruptions.

2.2 Proof for Assumption 2

It is shown in Section 5.4 of the main manuscript.

2.3 Proof for Assumption 3

Given input target domain $D_t = \{(\mathcal{X}_t, \mathcal{Y}_t)\}$, source domain $D_s = \{(\mathcal{X}_s, \mathcal{Y}_s)\}$, a corruption with 5 severity levels $T = \{t_i\}_1^5$, an ideal transfer loss function ℓ_{trans} and a DA model $m = f \circ c$, we first make some notions for precise:

Table 1. Average Shift of different corruptions

Corruption	Avg shift	Corruption	Avg shift
Gaussian Noise	0.22	Snow	0.25
Shot Noise	0.25	Elastic Transform	0.19
Impulse Noise	0.14	Contrast	0.26
Defocus Blur	0.08	Brightness	0.25
Motion Blur	0.13	JPEG Compression	0.04
Zoom Blur	0.12	Pixelate	0.05
Fog	0.24	Glass Blur	0.08
Frost	0.21		

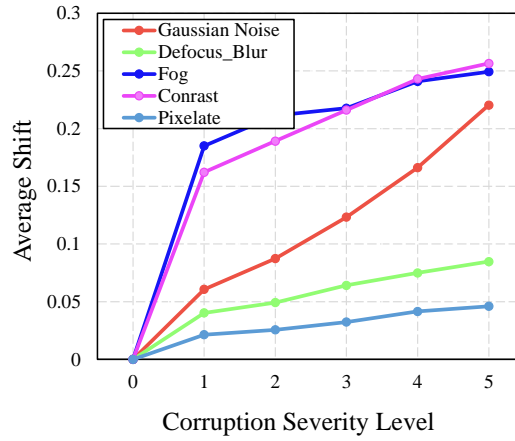


Fig. 2. Average Shift of different corruptions with 6 severity levels.

$$\begin{aligned}
\ell_{trans}(t_i) &= \mathbb{E}_{x_t \sim \mathcal{X}_t} [\ell_{trans}(f(t_i(x_t)), f(\mathcal{X}_s))], \\
Acc(t_i) &= \mathbb{P}_{(x_t, y_t) \sim D_t}(m(t_i(x_t)) = y_t), \\
\ell_{total}(t_i) &= \ell_{trans}(t_i) + \ell_{cls}(\mathcal{X}_s, \mathcal{Y}_s),
\end{aligned} \tag{2}$$

where $\ell_{trans}(t_i)$ denotes the average transfer loss of corrupted target domain samples. $Acc(t_i)$ denotes the classification accuracy of corrupted target domain samples. $\ell_{cls}(\mathcal{X}_s)$ denotes the classifier loss of source domain samples; $\ell_{total}(t_i)$ denotes the total loss of a classic DA models, which usually correlated to $Acc(t_i)$.

It is observed that the classification accuracy decreases as the increase of the severity level, as:

$$i < j \Rightarrow Acc(t_i) > Acc(t_j). \tag{3}$$

We make the proof by contradiction. If

$$\begin{aligned}
i < j &\Rightarrow \ell_{trans}(t_i) > \ell_{trans}(t_j) \\
&\Rightarrow \ell_{total}(t_i) > \ell_{total}(t_j),
\end{aligned} \tag{4}$$

the final classification accuracy should be $Acc(t_i) < Acc(t_j)$. Conflict with Equation (3).

3 PROOF FOR EQUATION (3) IN THE MAIN MANUSCRIPT

According to Assumption 1, $x_t^{(DDG)}$ and $t(x_t)$ are within the δ neighborhood $\{x | \|x - x_t\| \leq \delta\}$.

Table 2. mCE (%) for different parameters in TSCL-WC on the UDA task of Ar→Rw from Office-Home dataset.

object	δ	η	n	mCE (↓)
η	60/255	$> 2\delta$	2	48.0
	60/255	$> 2\delta$	10	49.6
	60/255	15/255	10	51.6
	60/255	6/255	10	52.8
δ	20/255	$> 2\delta$	2	49.5
	40/255	$> 2\delta$	2	48.6
	60/255	$> 2\delta$	2	48.0
	80/255	$> 2\delta$	2	47.3
	100/255	$> 2\delta$	2	47.2
	120/255	$> 2\delta$	2	46.9
n	140/255	$> 2\delta$	2	46.4
	60/255	$> 2\delta$	1	47.4
	60/255	$> 2\delta$	2	48.0
	60/255	$> 2\delta$	5	49.9
	60/255	$> 2\delta$	10	49.6

Suppose t_{max} as the most severe corruption in corruption set T . According to Assumption 3,

$$t_{max} = \arg \max_{t \in T} \ell_{trans} (f(t(x_t)), f(D_s)). \quad (5)$$

Due to the uncertainty of T , the corrupted versions $t(x_t)$ can be everywhere in δ neighborhood. Thus,

$$\begin{aligned} & \ell_{trans} (f(x_t^{(DDG)}), f(D_s)) \\ &= \ell_{trans} (f(t_{max}(x_t)), f(D_s)) = \ell_{max}. \end{aligned} \quad (6)$$

Suppose that

$$\begin{aligned} X^{(DDG)} &= \{x_t^{(DDG)} | \ell_{trans} (f(x_t^{(DDG)}), f(D_s)) = \ell_{max}\} \\ X^{(tm)} &= \{t_{max}(x_t) | \ell_{trans} (f(t_{max}(x_t)), f(D_s)) = \ell_{max}\}. \end{aligned} \quad (7)$$

We get

$$X^{(DDG)} = X^{(tm)}. \quad (8)$$

Thus, $x_t^{(DDG)} \in X^{(wc)}$ can represent $t_{max}(x_t) \in X^{(tm)}$, as:

$$x_t^{(DDG)} \Rightarrow t_{max}(x_t). \quad (9)$$

4 MORE ABLATION ON δ , η , AND n

Table 2 reports the mCE on different settings of hyper-parameter of DDG in Algorithm 2. Besides the conclusion of η in the main text, it is shown that the final corruption robustness improves as the increase of shift range δ and decrease of the update step n . For stability, we set $\delta = 60/255$, $\eta > 2\delta$ and $n = 2$ in this paper.

5 DETAILS OF CORRUPTIONS

We follow the same types of corruptions as Hendrycks *et al.* [?] proposed to investigate how neural networks are robust against to common corruptions and perturbations. The 15 types of corruptions are: Gaussian Noise, Shot Noise, Impulse Noise, Defocus Blur, Motion Blur, Zoom Blur, Fog, Frost, Snow, Elastic Transform, Contrast, Brightness, JPEG Compression, Pixelate, and Glass Blur. Fig. 3 illustrates examples of all the 15 kinds of corruptions. For each kind, there are 5 levels of severity as shown in Fig. 4.

6 OTHER DETAILS

Training details of Fig.5 of Section 5.3 in the main manuscript. All models are trained on a single domain (Real World of Office-Home). Given Gaussian Noise corruption set with five levels of severity $T = \{t_i\}_1^5$ (t_0 denotes clean images) and inputs x , the training details of the models are as follows.

- **Clean:** Supervised training on clean data.
- **All levels:** At the beginning of each iteration, we randomly select a corruption from $\{t_i\}_0^5$ to corrupt the inputs x . All corrupted inputs $t(x)$ are aligned with the original clean inputs x in feature space by contrastive loss.
- **Clean + Level 5:** At the beginning of each iteration, we randomly select a corruption from $\{t_0, t_5\}$ to corrupt the inputs x . All corrupted inputs $t(x)$ are aligned with the original clean inputs x in feature space by contrastive loss.
- **Level 5:** At the beginning of each iteration, we use level 5 corruption t_5 to corrupt the inputs x .



Fig. 3. Examples of 15 kinds of corruptions.

246
247
248
249
250
251
252
253
254
255
256
257
258
259
260
261
262
263
264
265
266
267
268
269
270
271
272
273
274
275
276
277
278
279
280
281
282
283
284
285
286
287
288
289
290
291
292
293
294

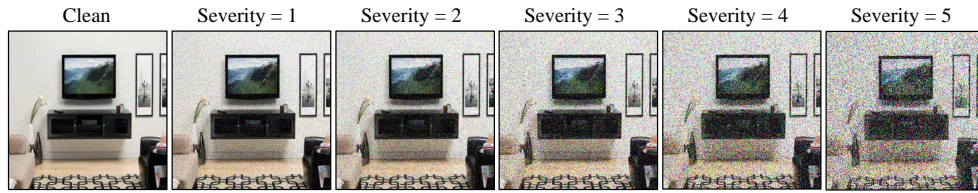


Fig. 4. Examples of 5 levels of severity.